A NEW TECHNIQUE OF SEARCHING FOR COSMIC-RAY ANTIPROTONS AND ANTIHELIUM

A. Buffington, Carl R. Pennypacker, Phil M. Lubin, and George F. Smoot

Space Sciences Laboratory and Lawrence Berkeley Laboratory,
University of California,
Berkeley, California 94720, USA

ABSTRACT

Current upper limits on the ratio of nucleonic antimatter to matter in the primary cosmic rays are about 10^{-4} for antiprotons and about 10^{-5} for heavier antimatter. Antiprotons should be observed at about 10^{-4}, due to inelastic cosmic-ray collisions in interstellar space. We describe a technique for significantly extending the search for these particles. The apparatus uses a Cerenkov counter, scintillators, and a thick, optically viewed lead-plate spark chamber. A selective trigger records only those events below Cerenkov threshold, but also penetrating the lead. Subsequent examination of the pictures removes residual contamination, yielding an acceptance window from about 60 to 320 MeV/nucleon in the apparatus. Corrections for the solar cavity's adiabatic deceleration should raise this energy window substantially.

1. Introduction

Cosmic rays are almost certainly a sample of material from beyond the solar system. The symmetry between matter and antimatter observed at accelerators suggests a Universe whose total baryon number is zero. If true, this would imply that somewhere there exist large amounts of antimatter. However, the bulk matter and antimatter must intermix only slightly, or the resulting annihilation gamma rays would create a flux greater than has been observed. Whatever barrier keeps matter and antimatter separated, possibly high-energy cosmic rays could penetrate it and reach us. These particles are the only practical means of our investigating these antimatter regions. Small amounts of antimatter can be made by high-energy collisions of cosmic rays with interstellar material, but this is negligible for nuclei heavier than antiprotons. Positrons and antiprotons are expected at fluxes of 10^{-3} and 10^{-4}, respectively, of the proton flux at the same energy (1,2). Positrons have been observed at about the expected flux, but only an upper limit exists for antiprotons (3,4). Searches for heavier antimatter have seen none in about 10^5 events examined (5,6).

Observation of a single, well-documented antihelium or anticarbon nucleus would be of great cosmological interest, since it would suggest the existence of fairly nearby regions of bulk antimatter. Antihelium could conceivably be left over from the Big Bang, but a heavier antinucleus such as anticarbon would have had to be synthesized in an antimatter star. Although not of cosmological significance, an antiproton flux is interesting as a secondary cosmic-ray constituent whose injection rate should be calculable from known parent proton fluxes, interstellar gas densities, and production cross-sections (2).

2. Technique and Apparatus

Previous cosmic-ray antimatter searches using emulsion stacks or magnetic spectrometers have been undiscriminating in their initial recording of data. These searches depended upon a detailed analysis of individual events to look for the characteristic signs of antimatter (direction of curvature in a magnetic field or annihilation prongs at the end of a stopping track). Although in

principle this technique could be substantially extended beyond present-day limits on the antimatter/matter ratio, it would be useful to employ a selective criterion in recording the data, to enrich the data sample in antimatter candidate events. In this paper, we describe such a selective criterion, which rejects normal matter events by an expected 1000:1 ratio, yet retains a reasonably high efficiency for recording antiproton and antihelium events. A detailed visualization of the events recorded provides the means for further background rejection.

Figure 1 shows the apparatus and the Table lists its specifications. A Cerenkov counter in the upper portion of the apparatus rejects incident particles above the Cerenkov threshold of 320 MeV/nucleon. Most particles below this threshold can penetrate only two-thirds or less through the lead-plate spark chamber in the lower portion of the apparatus, and thus cannot reach scintillator S_4, the final element of the trigger criterion. However, stopping antiproton or antihelium events have annihilation daughter pions which can frequently reach S_4, thus satisfying the trigger criterion. Upward-going annihilation pions may also register in the Cerenkov counter, but they do so too late to reject the event for the trigger criterion.

In another paper of this conference (OG-6-21), we discuss the various non-antimatter backgrounds which have been seen to meet this trigger criterion. Since none of these processes closely resemble antimatter annihilations when visualized in detail, they can be eliminated in the subsequent data analysis. It is necessary only that the trigger criterion reduce the apparatus trigger rate sufficiently that the photographic film (typically 35,000 frames) not be used up more quickly than the 20 hours hoped-for flight duration.

Once the trigger criterion has been met, the apparatus records spark locations in a thin spark chamber above the Cerenkov counter, and in the lead-plate spark chamber. The thin spark chamber is the same unit which we have flown in our magnetic spectrometer experiments (7). The lead-plate spark chamber is constructed of plates 2.1 mm thick, with 0.64 mm of aluminum glued on each side. Construction is identical to that of the lead-plate chamber used in our electron-positron experiment (8), except the plates are thicker and there are more of them. Multitrack efficiency for this chamber appears to be adequate for antiproton and antihelium detection. Lead was chosen for the plate material because of its favorable ratio of dE/dx to radiation length; the annihilation gamma rays shower and die out quickly compared with the charged pion track lengths, thus permitting a clear visualization of the charged-prong annihilation topology. Analysis of known background processes indicates that only a few background "antiprotons" should be expected in a balloon flight (comparable with expected atmospheric background) and negligible background antihelium.

Figure 2 shows the schematic diagram for the electronics. Pulses from the five experiment counters are photographed on a Hewlett-Packard 1744A storage oscilloscope along with the sparks. A small portion of the signal from S_2 is subtracted from the Cerenkov signal to remove, on the average, the small scintillation contribution in the Pilot 425 Cerenkov radiator. We have assumed this to be 3% of the relativistic signal (9). A top window, also imposed on S_2, removes triggers from nuclei heavier than helium, since these might meet the trigger criterion too easily with spallation neutrons and would in any case lie outside of the dynamic range of the pulse recording system. A dead time after each event allows for recharge of the spark-chamber capacitors, cycling of the oscilloscope, and winding the camera film.

RCA 8575 photomultipliers are used throughout to view the scintillators and Cerenkov counter. Two tubes view each scintillator, coupled through lucite-strip lightpipes. The light collection efficiency of these is typically 5%. The Cerenkov radiator is viewed by 24 phototubes, also coupled by lucite lightpipes, here providing about 20% collection efficiency. To reduce background

triggers from events with particle trajectories through lightpipes, the Cerenkov counter system almost completely surrounds S_2. Discriminator thresholds will be set at twice Z = 1 minimum ionizing for the top three scintillators, and at half Z = 1 minimum ionizing for S_4. The window discriminator on S_2 will reject events with more than 20 times Z = 1 minimum ionizing. The Cerenkov counter threshold will be set at about 3 photoelectrons.

The range of particle energy covered by the experiment is set by the Cerenkov threshold above, and sufficient penetration into the lead-plate spark chamber below. At the Cerenkov counter these limit the experiment to antiprotons and antihelium between 60 and 320 MeV/nucleon. For protons and helium-4 the fractional energy loss rates are identical. When energy losses in the top parts of the gondola and the expected 15 gm/cm^2 of residual atmosphere are included, the experiment covers roughly from 100 to 400 MeV/nucleon. Detection efficiency for antiprotons varies from 10% at the lowest energy to 50% at the highest, due to the varying coverage of S_4 and amount of intervening lead, for least- and most-penetrating antiproton events. Detection efficiency for antihelium should be greater because of the large number of annihilation prongs.

3. Interpretation

If the data flight from Canada (geomagnetic cutoff $\approx$ 0.5 GV/c) is fully successful, about 2 x 10^7 protons and 3 x 10^6 heliums below Cerenkov threshold should stop in the apparatus during the expected 20 hours of data-taking. This should allow observation of an antiproton flux as small as 10^{-6} of the proton flux, and a comparably small new antihelium/helium limit. Cross-sections for creating antiprotons nearly at rest in the laboratory frame are quite small, and an antiproton/proton ratio of about 10^{-6} might not be surprising for antiprotons of a few hundred MeV in interstellar space. However, the adiabatic deceleration of the solar cavity has the effect of raising the effective energy window of the experiment. Using a value of 200 MeV for this, the effective coverage is raised to 300 to 600 MeV/nucleon (10). The actual coverage should be wider because of a distribution of deceleration value rather than a fixed value for each event. Here, the calculations of Badhwar et al. (2) indicate an expected $\bar{P}/P$ ratio from 10^{-4} to 10^{-5}. Thus we expect to see between a hundred and a thousand antiprotons in this experiment. Moreover, since the adiabatic deceleration has not had a chance to act on antiprotons created nearby in the atmosphere, only a few of these should be observed in the experiment.

Recent theoretical speculations have suggested that the present-day matter-antimatter asymmetry in the Universe might be a consequence of baryon non-conserving reactions. The speculations fall into two classes. The first class couples violations of baryon-number conservation and CP invariance so that reactions in the very early fireball lead from symmetry to an excess of baryons. These speculations have some basis in some of the present day unified gauge theories of weak, electromagnetic, and strong interactions (11). The second class involves coupling violations of baryon number conservation and CPT invariance which would result in antiproton decay. Such speculation motivated the experiment which recently set a lower limit on the antiproton decay lifetime of 85 hours of storage in an accelerator ring (12). In the standard hot Big Bang model of the Universe, nearly all the protons and antiprotons would have annihilated each other away by 10^{-2} seconds from the initial singularity, therefore there must be a significant amount of decay of antiprotons by this time. By a significant amount we mean roughly $10^{-8\pm1}$ because that is the present ratio of protons to primordial photons whereas near the singularity the ratio must be near unity. Thus if antiproton decay created the present matter-antimatter asymmetry the antiproton decay lifetime must be on the order of $\tau_{\bar{p}} \approx 10^{6\pm1}$ sec $\approx 10^{1\pm1}$ days. It is evident that with such a short decay lifetime very few cosmic-ray-produced antiprotons would survive their typically 10^7 year galactic

travel time to be observed here at earth. Observation of the expected antiproton flux would establish an antiproton decay lifetime of the order of 10^7 years or greater, thus ruling out antiproton decay as a mechanism to explain the present matter-antimatter asymmetry in the Universe. Also it would provide a direct and strong test of CPT invariance.

References

1. Orth, C.D., and Buffington, A., Astrophys.J. 206, 312 (1976).
2. Badhwar, G.D., Golden, R.L., Brown, M.L., and Lacy, J.L., Ap. and Spc. Sci. 37, 283 (1975).
3. Buffington, A., Orth, C.D., and Smoot, G.F., Astrophys.J. 199, 669 (1975).
4. Badhwar, G.D., Golden, R.L., Lacy, J.L., Zipse, J.E., Daniel, R.R., and Stephens, S.A., Nature 274, 137 (1978).
5. Smoot, G.F., Buffington, A., and Orth, C.D., P.R.L. 35, 258 (1975).
6. Steigman, G., Annual Rev. of Astr. and Ap. 14, 339 (1976).
7. Smith, L.H., Buffington, A., Wahlig, M.A., and Dauber, P., R.S.I. 43, 1 (1972).
8. Buffington, A., Orth, C.D., and Smoot, G.F., Nucl. Inst. and Meth. 122, 575 (1975).
9. Ahlen, Steven P., Ph.D. thesis (unpublished), University of California, Berkeley, September 1976.
10. Garcia-Munoz, M., Mason, G.M., and Simpson, J.A., Astrophys.J. 197, 489 (1975).
11. Yoshimura, M., P.R.L. 41, 281 (1978).
12. see, for example, Science News 114, 132 (1978).

TABLE OF APPARATUS SPECIFICATIONS (PRELIMINARY)

Scintillator S_1	1.00 x 1.00 meters by 1.0 cm thick, Pilot Y
Scintillator S_2	0.89 x 0.87 meters by 1.0 cm thick, Pilot F
Scintillator S_3	0.70 x 0.70 meters by 1.0 cm thick, Pilot F
Scintillator S_4	0.74 x 0.74 meters by 1.0 cm thick, Pilot F
Cerenkov radiator	0.92 x 0.92 meters by 1.3 cm thick, Pilot 425
Top Spark Chamber	1.0 x 1.0 meters, laminated foam and aluminum foil 4 gaps, 0.34 gm/cm^2 thick, optically viewed.
Lead Spark Chamber	Top 4 gaps, 0.5 cm each, 1.5 mm thick aluminum plates 50 gaps, 0.5 cm each, 2.55 gm/cm^2 laminated Pb-Al 1.3 cm steel plate between lead spark chamber & S_4. Active area is 70 x 70 cm, thickness is 47.6 cm.
Geometry factor	0.6 m^2 ster, by Monte Carlo calculation, excluding S_4.

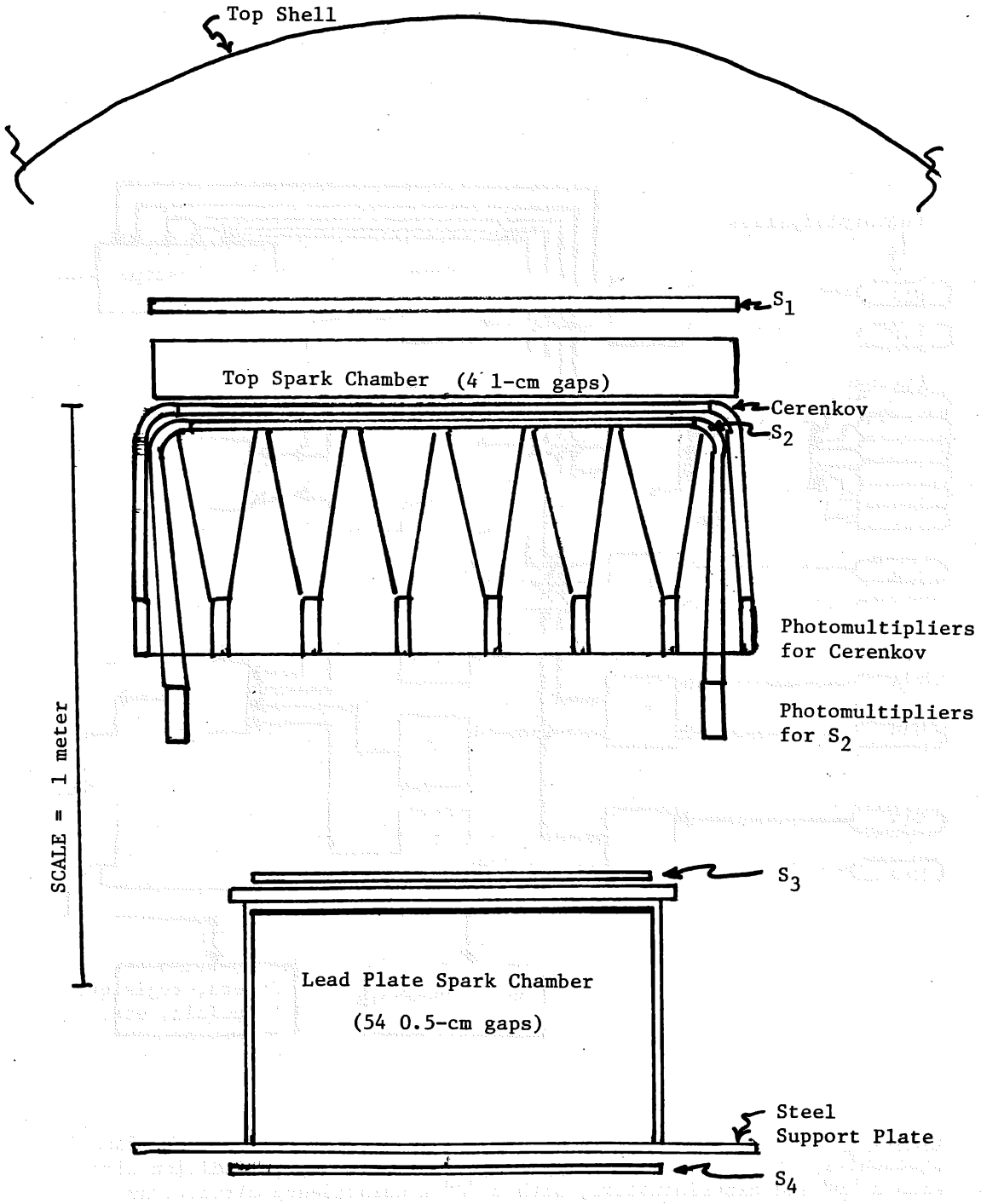

FIGURE 1. Schematic diagram of the apparatus. The pressure shell completely encloses the experiment within two hemispheres. Lightpipes have been shown only for the Cerenkov counter and scintillator S_2.

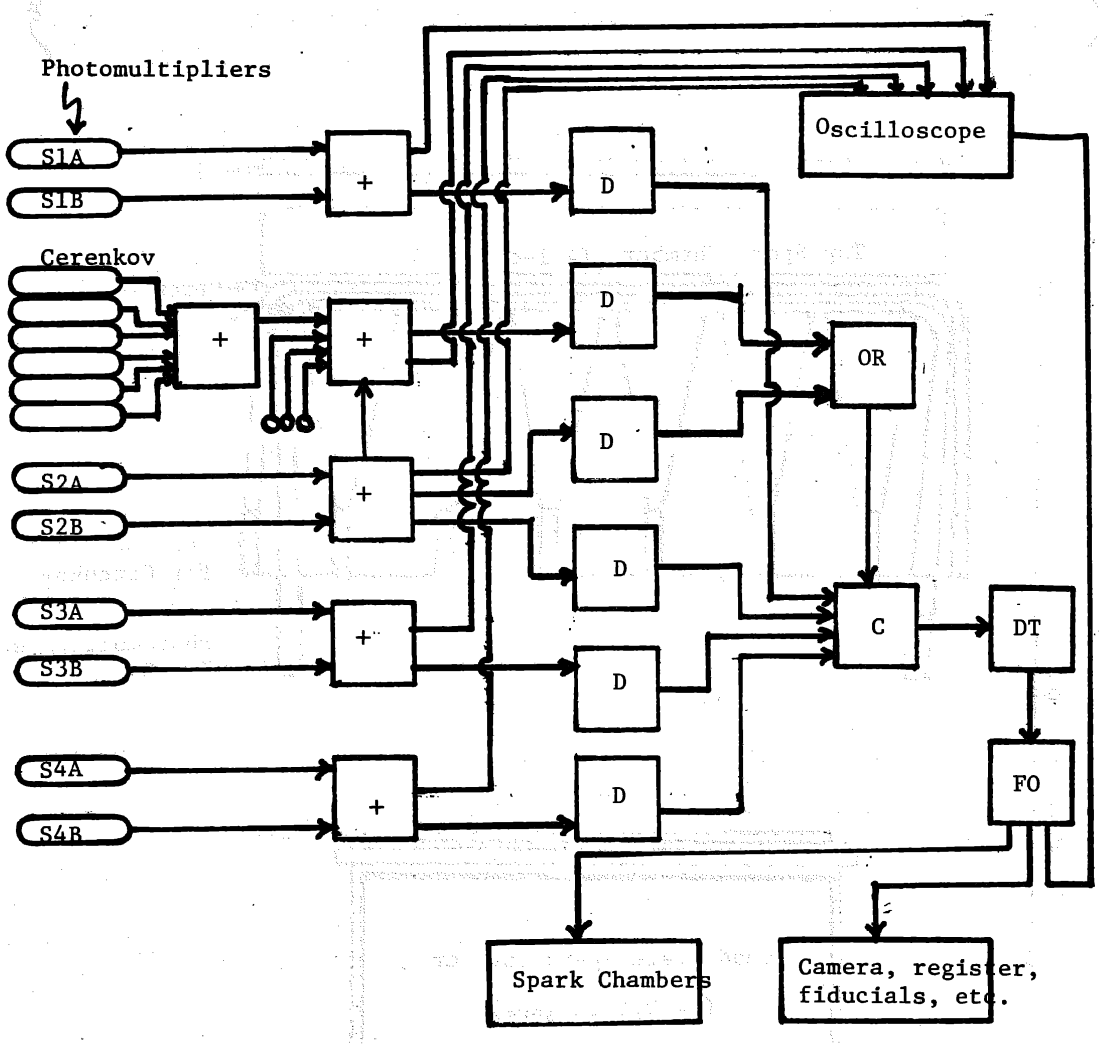

Figure 2. Schematic electronics diagram. Only six of the twenty-four Cerenkov photomultipliers are shown. Boxes with a "+" are analog addition circuits, with a "D" are discriminators, with a "C" a coincidence circuit, an "OR" a logic-level adder, "DT" a dead-time circuit, and "FO" a logic-level fanout.